Alternate Air Bearing Slider Designs for Areal Density of 1 Tb/in^2

Jia-Yang Juang, Du Chen, and David B. Bogy, *Fellow, IEEE*

Computer Mechanics Laboratory, Department of Mechanical Engineering, University of California at Berkeley, Berkeley, CA 94720 USA

To achieve the areal density goal in hard disk drives of 1 Tb/in^2 the minimum physical spacing or flying height (FH) between the read/write transducer and disk must be reduced to about 2 nm. At such low spacing new nanoscale forces act between the slider and disk, such as intermolecular and electrostatic forces, which must be taken into consideration in the air bearing design. These forces increase the level of flying height modulations (FHMs), which in turn creates dynamic instability and intermittent contact in the flying head slider similar to what has been observed in experiments. Here, we present three possible approaches to minimize such forces and/or reduce FHM by FH control, including a micro-trailing pad slider, a thermal flying height control slider, and a piezoelectric flying height control slider for hard disk drives.

Index Terms—Air-bearing surface (ABS), electrostatic forces, flying height (FH), flying height modulation (FHM), head-disk interface, inter-molecular forces, piezoelectric flying height control, thermal flying height control (TFC).

I. INTRODUCTION

AS THE spacing between the slider and the disk decreases in hard disk drives, the linear bit spacing of the magnetic recording can decrease, resulting in higher areal density. According to the Wallace spacing loss equation, the magnetic signal increases exponentially as the distance decreases between the magnetic media and the transducer. The maximum magnetic signal can be obtained at a spacing of zero, resulting in a contact recording scheme. However, there are tradeoffs between reducing the bouncing vibration and wear in such systems [1]. Another significant concern is the thermal stability of both the media and GMR sensors. The read-back signal of GMR sensors can be significantly affected by thermal influences since their electrical resistance is temperature dependent. Continuous high-speed contact generates excessive heat, which undermines the recording performance. The above issues have to be addressed before a reliable contact recording system can be realized.

Instead of contact recording, we consider a flying scheme, in which the nominal mechanical spacing (or flying height, FH) between the slider and the disk is reduced to about 2 nm in order to achieve an areal density of 1 Tb/in^2. On the other hand, due to this reduction in spacing between the slider and the disk, the threshold of new nanoscale phenomena will be crossed. In particular, short range forces between the slider and disk come into play, such as intermolecular and electrostatic forces.

A study of the effect of intermolecular forces and electrostatic forces was presented in previous papers, e.g., [2]. The intermolecular and electrostatic forces do not have a significant effect on the flying characteristics of high flying sliders (spacings greater than 10 nm), but they become increasingly important at low spacings (below 5 nm). These forces are attractive in nature and hence result in a reduction in fly height as compared to what would be the case without them. It is also found that these highly nonlinear forces increase the level of disk morphology induced FHM, which in turn creates dynamic instability and intermittent contact in the flying head slider.

Some indications of dynamic instability have been observed experimentally for ultra-low-flying sliders, such as different take-off and touch-down disk speeds (hysteresis) for flying sliders [3]. Various models have been used to explain the instability that results from the intermolecular forces and charge buildup at the HDI. With the decrease in the head-media spacing (HMS) in order to achieve higher areal density the contribution of intermolecular and electrostatic forces to the force balance at the HDI can no longer be neglected. Hence, it is important to investigate alternate air bearing slider designs that can minimize nanoscale short range forces and/or reduce FHM by FH control. To minimize these forces, the area of the sliders in close proximity of disks has to be reduced. This can be achieved by reducing the size of central trailing pads or using higher flying sliders with actuation that can move the read/write transducer closer to the disk on demand. To reduce the FHM by FH control, the bandwidth of actuation has to be high enough to compensate the air bearing dynamics.

In this paper, we present three alternate approaches to sustain a more stable HDI for low (transducer) FH sliders, including a micro-trailing pad slider, a thermal flying height control slider (TFC), and a piezoelectric flying height control slider for hard disk drives. This paper is organized as follows. First, a passive air bearing surface (ABS) slider with a micro-trailing pad was designed and its static and dynamic performances were simulated by an ABS Reynolds equation solver (CML Air Bearing Simulation program, CMLAir). In the second part of the paper, a TFC slider with an additional heating element near the read/write transducer is presented. Finite-element analysis and CMLAir were used to predict the magnitudes of thermal protrusion, FH reduction, inter-molecular forces, actuation bandwidth, and power consumption. Then, the actuation bandwidth of a piezoelectric slider was calculated by finite-element analysis and measured by laser Doppler vibrometer (LDV). Further, the advantages and disadvantages of these three solutions are discussed.
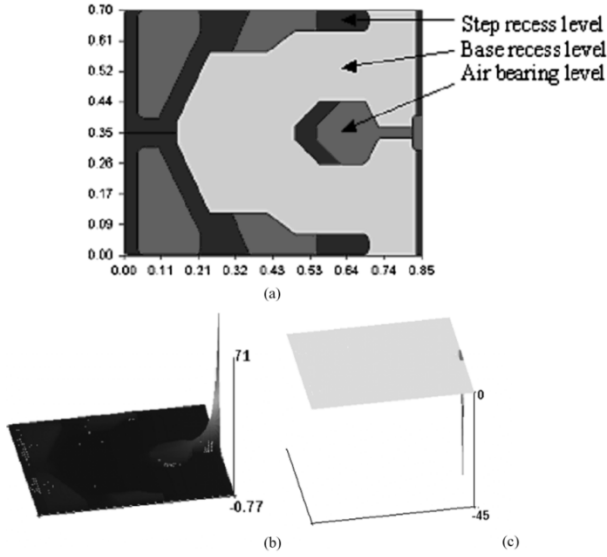
Fig. 1. (a) Air bearing surface design. (b) Air bearing pressure profile. The scale displayed is normalized to ambient pressure: $(p - p_a)/p_a$. (c) Intermolecular adhesion pressure profile (unit: kg/m^2).

TABLE I
AIR BEARING SPECIFICATIONS AND STATIC FLYING ATTITUDES

Slider Size: 0.85×0.7×0.23 mm3
Crown: 18 nm
Camber: 2.5 nm
Suspension Load: 0.8 gf
Disk RPM: 10000
Hamaker const: A=1×10^{-19} J, B=1×10^{-76} Jm^6

Radial Position (mm)	22.9	17.1	15	12	11.4
Skew (°)	6.65	1.1	0	-5	-6.65
Pitch (µrad)	243.50	210.84	196.68	172.06	165.11
Roll (µrad)	-5.61	-6.96	-7.35	-8.03	-8.65
Transducer FH (nm)	2.05	2.28	2.20	2.32	2.71
Minimum FH (nm)	0.72	1.08	0.96	1.53	0.81
Intermolecular Force (gf)	**0.026**	**0.190**	**0.195**	**0.136**	**0.179**
Negative Force (gf)	1.656	1.534	1.464	1.332	1.300

II. THREE APPROACHES FOR FLYING SLIDERS

A. Micro-Trailing Pad Slider

1) Air Bearing Surface (ABS) Design: Due to the similarity of the effects of intermolecular forces and electrostatic forces [2] on the slider's static and dynamic performance, we consider only the intermolecular force in the following numerical studies. To reduce the short range attractive forces between the slider and disk the trailing pad of this 2-nm flying height femto slider is reduced to a micro size. The ABS design is shown in Fig. 1 with a close approach trailing pad of 100 µm × 25 µm. The transducer is centered at the location (0.84 mm, 0.35 mm) near the trailing edge center. The ABS is designed with the considerations of high stiffness, ease of manufacturing and constant FH from inner diameter (ID) to outer diameter (OD). Simulation results for the transducer flying height (FH) from OD to ID are shown in Table I. As seen, the FH is between 2 and 3 nm.

TABLE II
MODAL FREQUENCIES AND DAMPING RATIOS

Radius Posi. (mm) and skew (°)	Mode 1		Mode 2		Mode 3	
	Freq. (kHz)	Damping Ratio (%)	Freq. (kHz)	Damping Ratio (%)	Freq. (kHz)	Damping Ratio (%)
22.9, 6.65	79.55	2.44	130.83	4.37	132.86	4.42
17.1, 1.1	129.68	2.86	131.52	2.91	139.29	5.88
15, 0	108.75	6.40	133.19	2.80	135.50	2.90
12, -5	136.44	5.13	140.08	4.83	145.53	5.13
11.4, -6.65	134.96	2.17	144.35	3.33	198.42	1.32

The intermolecular force is much smaller than the negative air bearing force. At the OD position the intermolecular force is much smaller while the FH is also smaller due to higher pitch. For a conventional ABS with 1 nm minimum FH the intermolecular force is around 0.6 gf [3]. Compared with the conventional slider, the micro-trailing pad slider greatly reduces the effect of intermolecular adhesion.

Fig. 1(b) and (c) shows the air bearing pressure profile (normalized by the ambient pressure) and the intermolecular adhesion pressure profile (unit: kg/m^2), respectively, at the zero skew position. For different radius positions the pressure profile geometry remains relatively constant with differences only in the amplitudes of the pressures. Due to the close approach of the trailing pad, both the air pressure and the intermolecular adhesion pressure are much higher on the micro-trailing pad than on the other air bearing pads. Correspondingly, the stiffness in the roll motion is inevitably low and the roll angle varies from ID to OD, which is also shown in Table I.

2) Dynamic Analysis: To maintain a reliable head-disk interface, the air bearing slider needs to keep the contacts between slider and disk to a minimum, although intermittent contacts are inevitable when the FH is similar to the disk roughness. So the dynamics performance of the air bearing slider is important. The more stable the air bearing slider, the less damage will be caused by contact and the faster the slider will return its steady state after being disturbed. The CML Dynamics Air Bearing Simulator solves the generalized Reynolds equations coupled with the dynamics of the slider body and a lumped parameter suspension, where the suspension force is represented by flexure stiffness and damping coefficients. Using the simulator we can obtain simulations of the dynamic response of the nonlinear air bearing slider system for various inputs. Linear modal analysis and the system identification method (CML PIP program) can alos be used to obtain the modal parameters of the air bearing slider system with small perturbations about the slider's steady flying attitude. By simulating the response of the slider to initial velocities in the pitch, roll, and vertical directions, we can estimate the impulse response functions, perform modal analysis, and obtain the modal stiffness, damping ratios, and nodal lines [4]. The interface is more stable when the frequencies and the damping ratios are higher. The modal frequencies and damping ratios are shown in Table II for the micro-trailing pad slider at various radius positions. Mode 1, Mode 2, and Mode 3 correspond to the three coupled modes, i.e., roll, first-pitch and

TABLE III
PLOTS OF TRANSDUCER FLYING HEIGHT VERSUS TIME FOR THE SLIDER AT
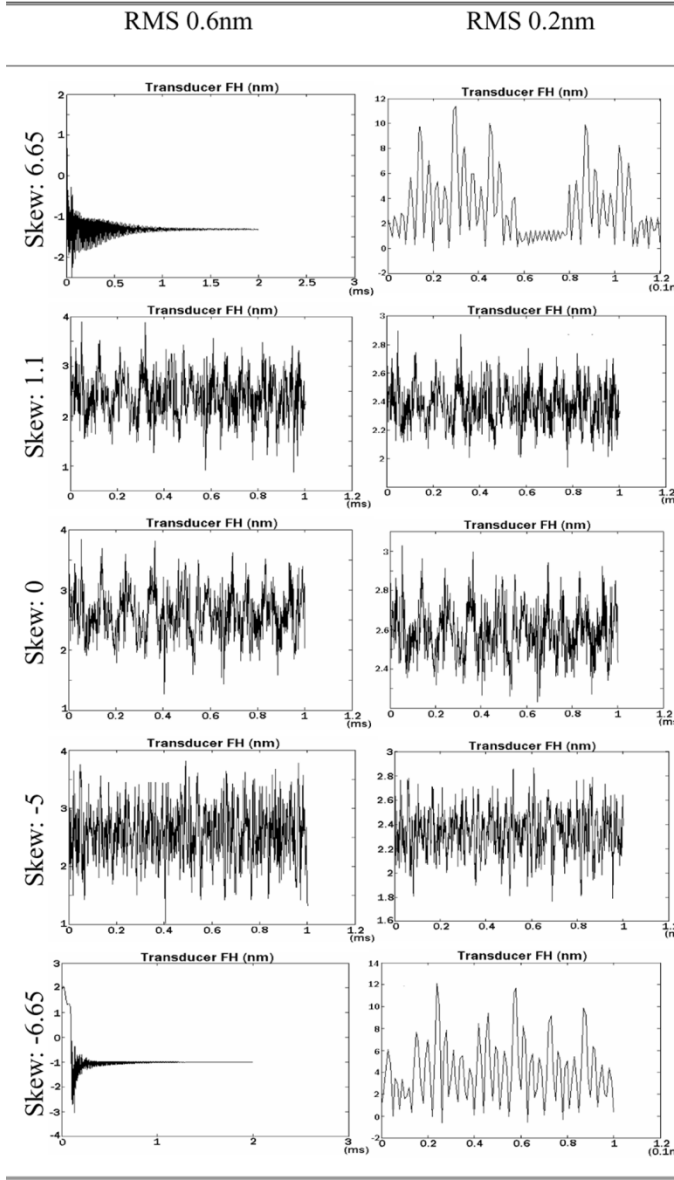VARIOUS SKEW ANGLES ON TWO MEASURED DISK SURFACES

Fig. 2. Finite-element model of a TFC slider.

TABLE IV
MATERIAL PROPERTIES USED IN THE FEA

Layer and Material		Young's modulus (GPa)	Thermal conductivity (W/m.K)	Coefficient of thermal expansion (x 10^{-6}/ °C)	Poisson's ratio
Slider substrate	Al$_2$O$_3$-TiC	390	20	7.1	0.22
Under-coat (1.2 μm)	Al$_2$O$_3$ (thin layer)	138	1.8	7.8	0.25
Shields (2.0 μm)	Ni-Fe	200	35	12.8	0.3
Bottom pole (1.0 μm)	Ni-Fe	200	35	12.8	0.3
Coil (2 μm)	Cu	130	400	15.4	0.34
Heater (250 nm)	Ni-Fe (thin layer)	200	30	12.8	0.3
Coil insulation (5 μm)	Photo-resist	7	0.209	51	0.2
Top pole (1.0 μm)	Ni-Fe	200	35	12.8	0.3
Over-coat (23 μm)	Al$_2$O$_3$	138	25	7.8	0.25

mance at the OD and ID is still questionable. This is consistent with the conclusion of Thornton and Bogy [6]. Although the intermolecular force is small at the ID and OD the slider is more likely to contact the disk there due to larger pitch and roll angles. The HDI needs optimizing further so that the air bearing slider does not contact the disk.

B. Thermal Flying Height Control (TFC) Slider

1) Numerical Analysis: The concept of controlling transducer flying height by the thermal expansion of materials was first demonstrated by Meyer *et al.* [7], in which a resistance heating element (heater) was mounted to the slider body and a temperature sensor was used for sensing an operating temperature of the slider body. When a current is applied through the heater a portion of the head protrudes due to the mismatch of the coefficients of thermal expansion of the various materials. Such protrusion reduces the FH. However, little has been published about how much the short range forces can be diminished and how fast such actuation can respond at flying conditions.

In order to determine the magnitudes of these forces and the bandwidth, a finite-element model of a TFC slider was created as shown in Fig. 2. The heating element, coil, write poles, shields, photoresist layer, undercoat insulation layer, and over-coat were modeled in detail to study the effects of the heating power on the flying attitude. The material properties and thick-

second-pitch. Due to the smaller gap between the slider and disk, the modal frequencies are higher than those of some other sliders with sub-5 nm FH [5]. But the damping ratios are similar.

The spacing fluctuation between the transducer and the disk, or flying height modulation (FHM) is another important phenomenon and it also needs be held to a minimum. Again, using the CML Dynamics Air Bearing Simulator we obtained the results in Table III, which show the transducer FHM of the slider on two measured disk surfaces, the RMSs of which were 0.6 and 0.2 nm, respectively.

These results reveal that on the rougher disk surface (RMS 0.6 nm) the FHM is about 2 nm when the skew angle is 0, 1.1° or −5°. However, when the skew angle is ±6.65° the slider is in contact with the disk. On the smooth disk (RMS 0.2 nm), the FHM is less than 1 nm when the skew angle is 0, 1.1° or −5°. But when skew angle is ±6.65°, the slider bounces on the smooth disk. This indicates that the slider's dynamic perfor-
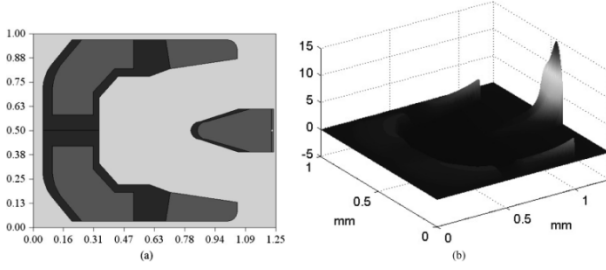
Fig. 3. (a) An ABS design used in this study. (b) The air pressure distribution of this ABS. The scale displayed is normalized to ambient pressure: $(p - p_a)/p_a$.
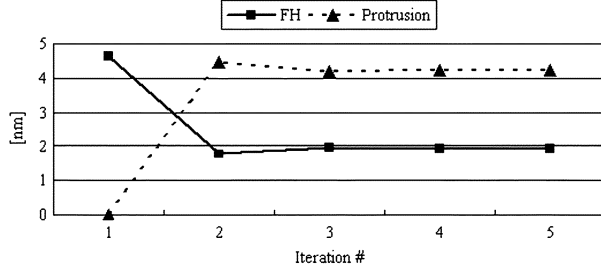

Fig. 4. Steady-state FH and thermal protrusion were obtained after several numerical iterations at a heating power of 30 mW.

TABLE V
COMPARISON OF FLYING ATTITUDES

	Protrusion (nm)	FH (nm)	Pitch (μrad)	Roll (μrad)	IMF (gf)	Max. pressure (atm)
Before protrusion	0	4.62	215	0.7	**0.037**	16
After protrusion	4.2	1.96	212	0.4	**0.065**	30

ness of each layer are shown in Table IV. The thermal conductivities of thin layers are higher than the bulk values due to the heat carrier-boundary scattering and the altered microstructure of thin films [8].

The cooling effect of the air bearing plays a key role in this 3-D heat transfer problem. We first used CMLAir to obtain the nominal FH, pitch, roll, and air pressure distribution of a 5-nm FH ABS slider as shown in Fig. 3. The effect of intermolecular forces was included with a nominal value of the Hamaker constant (A = 1×10^{-19} J). Then we calculated the heat flux through the air bearing based on the model developed by Chen *et al.* [9]. The temperature distributions and pole-tip protrusions were then calculated based on the model and boundary conditions. Since the thermal protrusion causes deformation of the ABS and hence changes the flying attitudes, an iteration approach is used to obtain an equilibrium solution.

2) Results and Discussions: Fig. 4 shows that the steady-state FH and thermal protrusion were obtained after several numerical iterations at a heating power of 30 mW. The disk rotational speed, radial position of the head, and skew angle were 7200 rpm, 23 mm, 9.1°, respectively. The FH was reduced from 4.62 to 1.96 nm with a thermal protrusion of 4.2 nm. The ratio of FH reduction to protrusion was 63%. The loss of 37% FH reduction was mainly attributed to the increased lift force and the reduced pitch angle as shown in Table V. More importantly, the intermolecular force (IMF) was found to be much smaller than
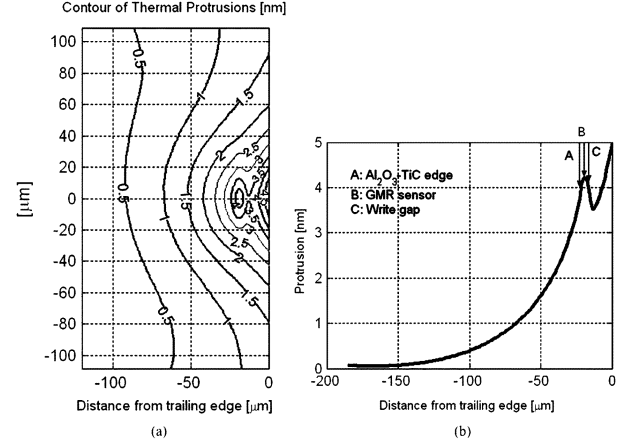

Fig. 5. Thermal protrusion profiles on the ABS (a) and along the center line across the read/write transducer.
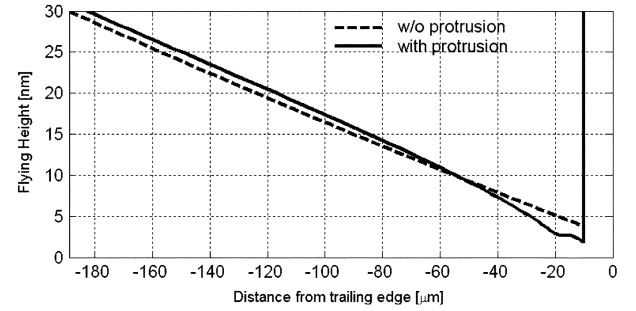

Fig. 6. Comparison of FH profiles along the center line of ABS. The distances of the write gap and GMR sensor from the trailing edge are 16.3 and 19.8 μm, respectively.
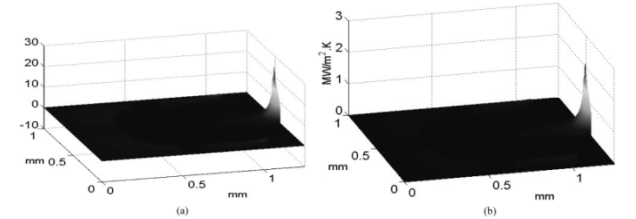

Fig. 7. Air pressure distribution (a) and the distribution of heat transfer film coefficient on the ABS with thermal protrusion.

that of conventional sliders with similar FHs due to the fact that only a small region of the slider was protruded in the proximity of the disk.

The protrusion profiles on the ABS and along the center line across the read/write transducer are shown in Fig. 5(a) and (b), respectively. Fig. 6 shows the FH reduction along the center line of the ABS. In the case with thermal protrusion, the air pressure near the read/write transducer significantly increases and this lifts the slider upwards, reducing the pitch angle. This highly concentrated air pressure induces extremely high heat flux through the air bearing surface as shown in Fig. 7.

Fig. 8 shows the temperature distribution over the ABS and around the read/write transducer at a heating power of 30 mW. A temperature valley is observed near the read/write element, which is caused by the extremely concentrated pressure effect on the heat transfer in the air bearing. A similar "butterfly shape" of temperature distributions was experimentally measured by
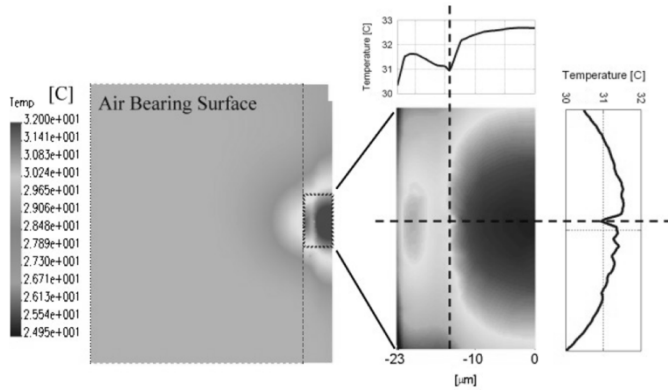
Fig. 8. Temperature distributions of a flying slider with thermal protrusion at a heating power of 30 mW. Line distributions show a clear temperature valley near the read/write head.
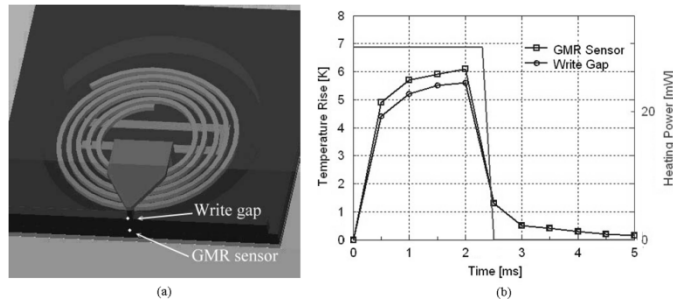

Fig. 9. Transient temperature changes of a flying slider with a varying heating power.

Xu *et al.* [10]. A lower temperature increase is beneficial for GMR sensors which are sensitive to temperature variation.

A transient thermal study was conducted to investigate the bandwidth of TFC sliders. The power to the heating element was set to 30 mW from 0 to 2.3 ms and was turn off at 2.5 ms. The temperature changes of both the GMR sensor and write gap were monitored as shown in Fig. 9. It requires about 1 ms for the read/write transducer to reach its steady-state values, corresponding to a bandwidth of 1 kHz. This is too slow for active control of FHM.

C. Piezoelectric Flying Height Control Slider

The bandwidth of TFC sliders is much lower than the air bearing frequencies, which may be up to 200 kHz. For this reason TFC sliders have little control over FHM and other dynamic losses of FH. The inherent high power consumption of thermal actuation also limits the stroke of protrusions. Several research groups [11]–[15] have presented the FH control using a piezoelectric unimorph cantilever actuator. Some of their results were summarized in Table VI. However, their studies were focused on compensating for static spacing loss caused by design tolerances and ambient pressure changes. Neither short ranges forces nor suppression of FHM was considered. Liu *et al.* [16] investigated an active FH control method for suppressing FHM by bonding a layer of piezoelectric film on one side of the suspension and using real-time spacing variation signals derived from the read-back signal as feedback. However, the short range

TABLE VI
COMPARISON OF THREE APPROACHES

|	Micro-trailing pad slider	Thermal quasi-static control slider	Piezoelectric dynamic control slider
FH control or adjustment	N/A	Yes (thermal expansion)	Yes (piezoelectricity)
Intermolecular forces	Minimize (0.19 gf)	Minimize (0.065 gf)	Compensate (0.03 gf [17], [18])
Actuation bandwidth	N/A	Low (1 kHz)	High (610 kHz; > 100 kHz [13]; 700 kHz [14]; 243 kHz [15])
Actuation displacement (non-flying condition)	N/A	Low (0.14 nm/mW)	High (9 nm/V [12]; 17.5 nm/V [13] 15 nm/V [14]; 1.5 nm/V [15])
Power consumption	N/A	High (30 mW)	Low
Manufacturing complexity	Low	Medium	High
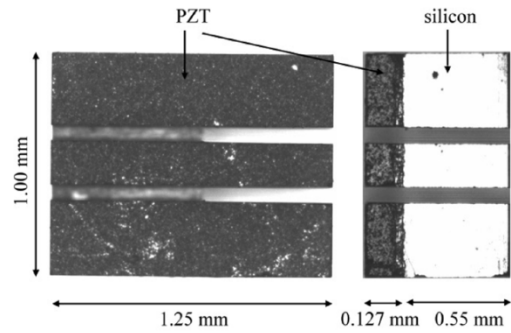
Fig. 10. A piezoelectric pico-slider used to determine the actuation bandwidth.

forces were not considered and since the active element was located on the suspension, the bandwidth was limited by the suspension dynamics.

Juang and Bogy designed a nonlinear compensator for piezoelectric sliders for dynamic active control of FH [17], [18] in the presence of short range forces, where the piezoelectric unimorph cantilever was used as actuator and the read-back signal was used as feedback. In order to suppress the FHM due to the air bearing dynamics, an actuation bandwidth of 400 kHz may be required. There is no inherent frequency limit for piezoelectric materials. In practice the frequency limits of application are usually determined by resonances associated with the physical structure of actuators. In order to investigate the resonance frequencies of piezoelectric sliders, we attached a 127 μm thick PZT layer on a silicon pico-slider as shown in Fig. 10. It was then bonded on a substrate and an LDV apparatus was used to measure the vibration of the cantilever as illustrated in Fig. 11(a). Sinusoidal voltages with frequencies from 0 to 1 MHz were applied to the central PZT layer. The first observed resonance frequency was about 610 kHz.

A finite-element analysis was also carried out for comparison. The results show that the first natural frequency is about 470 kHz for two different boundary conditions as shown in Fig. 12. The higher value of the measured frequency may be caused by an
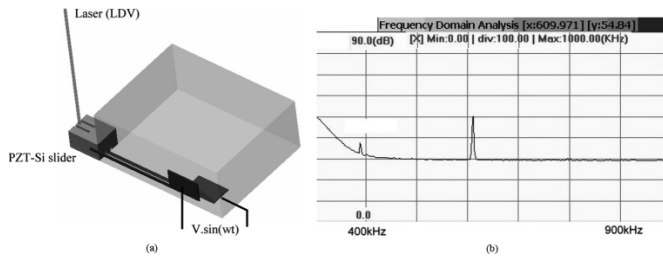
Fig. 11. (a) Experimental setup. (b) The first measured resonance frequency is about 610 kHz.
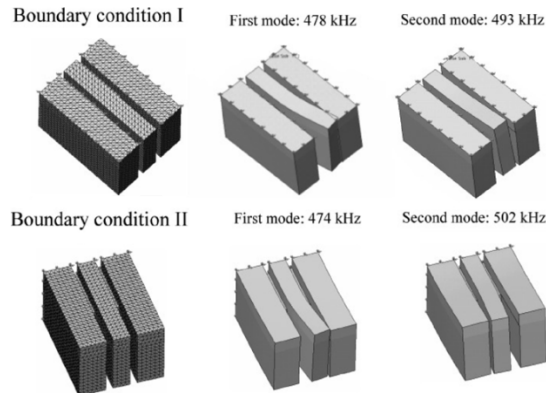

Fig. 12. Finite-element models and the first two modes and natural frequencies for two different boundary conditions.

amount of epoxy dispensing on the slider body in the experimental setup.

III. DISCUSSIONS

A brief summary of the advantages and disadvantages for each approach is given in Table VI. The quantitative values may vary from one design to another but the qualitative properties should be the same. It is found that the intermolecular forces at a transducer FH of 2 nm were reduced in all three approaches. Since the micro-trailing pad slider does not have the ability of FH control, it may lose flying stability when there are static and/or dynamic spacing loss. The thermal protrusion of TFC sliders can be controlled by adjusting the power of heating elements but the inherent power-consuming thermal actuation limits the actuation displacement, especially for mobile applications. The quasistatic FH control allows TFC sliders to compensate the static spacing loss. The piezoelectric dynamic control slider shows promising performance of higher bandwidth, larger actuation displacement, and higher power efficiency. However, the requirement of piezoelectric materials and modification of the slider design poses challenges in integration of the fabrication process and increases the manufacturing cost.

IV. CONCLUSION

While nanoscale design has been used in hard disk drives for several years, only recently have new phenomena arisen that are associated with nanoscale dimensions. As the hard disk drive industry advances toward the areal density of 1 Tb/in^2 the physical spacing between the air bearing slider that carries the read/write transducer and the top surface of the magnetic disk will be reduced to ~2 nm. In this spacing range new forces, such as in-

termolecular and electrostatic forces, act and can increase the level of FHM and cause dynamic instability of the flying head slider. Three possible approaches were studied to minimize such forces for flying sliders, including a micro-trailing pad slider, a thermal quasistatic control slider, and a piezoelectric dynamic active control slider for hard disk drives. The advantages and disadvantages for each one are also discussed.

REFERENCES

[1] M. Yanagisawa, A. Sato, K. Ajiki, and F. Watanabe, "Design concept of contact slider for high-density recording," *Electron. Commun. Jpn.*, pt. 2, vol. 80, no. 2, pp. 43–48, 1997.
[2] V. Gupta and D. B. Bogy, "Dynamics of sub-5 nm air bearing sliders in the presence of electrostatic and intermolecular forces at the head disk interface," *IEEE Trans. Magn.*, vol. 41, no. 2, pp. 610–615, Feb. 2005.
[3] R. Ambekar, V. Gupta, and D. B. Bogy, "Experimental and numerical investigation of dynamic instability in head disk interface at proximity," *ASME J. Tribol.*, vol. 127, pp. 530–536, 2005.
[4] Q. H. Zeng and D. B. Bogy, "Stiffness and damping evaluation of air bearing sliders and new designs with high damping," *ASME J. Tribol.*, vol. 121, pp. 341–7, 1999.
[5] B. H. Thornton and D. B. Bogy, "A numerical study of air-bearing slider form-factors," *ASME J. Tribol.*, vol. 126, pp. 553–8, 2004.
[6] ——, "Head-disk interface dynamic instability due to intermolecular forces," *IEEE Trans. Magn.*, vol. 39, no. 5, pp. 2420–2422, Sep. 2003.
[7] D. W. Meyer, P. E. Kupinski, and J. C. Liu, "Slider With Temperature Responsive Transducer Positioning," U.S. Patent 5 991 113, Nov. 23, 1999.
[8] Y. Yang, S. Shojaeizadeh, J. A. Bain, J. G. Zhu, and M. Asheghi, "Detailed modeling of temperature rise in giant magnetoresistive sensor during an electrostatic discharge event," *J. Appl. Phys.*, vol. 95, pp. 6780–6782, 2004.
[9] L. Chen, D. B. Bogy, and B. Strom, "Thermal dependence of MR signal on slider flying state," *IEEE Trans. Magn.*, vol. 36, no. 5, pp. 2486–2489, Sep. 2000.
[10] J. Xu, M. Kurita, and M. Tokuyama, "Thermal analysis of a magnetic head," *IEEE Trans. Magn.*, vol. 40, no. 4, pp. 3142–3144, Jul. 2004.
[11] C. E. Yeack-Scranton, V. D. Khanna, K. F. Etzold, and A. P. Praino, "An active slider for practical contact recording," *IEEE Trans. Magn.*, vol. 26, no. 5, pp. 2478–2483, Sep. 1990.
[12] M. Kurita and K. Suzuki, "Flying-height adjustment technologies of magnetic head sliders," *IEEE Trans. Magn.*, vol. 40, no. 1, pp. 332–336, Jan. 2004.
[13] K. Suzuki, R. Maeda, J. Chu, T. Kato, and M. Kurita, "An active head slider using a piezoelectric cantilever for in situ flying-height control," *IEEE Trans. Magn.*, vol. 39, no. 2, pp. 826–831, Mar. 2003.
[14] N. Tagawa, K. Kitamura, and A. Mori, "Design and fabrication of MEMS-based active slider using double-layered composite PZT thin film in hard disk drives," *IEEE Trans. Magn.*, vol. 39, no. 2, pp. 926–931, Mar. 2003.
[15] L. Su, M. Kurita, J. Xu, K. Kato, K. Adachi, and Y. Miyake, "Static and dynamic characteristics of active-head sliders," *Tribol. Int.*, vol. 38, pp. 717–723, 2005.
[16] X. Liu, A. Li, W. Clegg, D. F. L. Jenkins, and P. Davey, "Head-disk spacing variation suppression via active flying height control," *IEEE Trans. Instrum. Meas.*, vol. 51, no. 5, pp. 897–901, Oct. 2002.
[17] J. Y. Juang and D. B. Bogy, "Design of controlled flying proximity sliders for head-media spacing variation suppression in ultra-low flying air bearings," *IEEE Trans. Magn.*, vol. 41, no. 10, pp. 3052–3054, Oct. 2005.
[18] ——, "Nonlinear compensator design for active sliders to suppress head-disk spacing modulation in hard disk drive," *IEEE/ASME Trans. Mechatronics*, to be published.